Available online at www.sciencedirect.com
SCIENCE DIRECT®
Advances in Space Research 36 (2005) 2012–2020
ADVANCES IN SPACE RESEARCH (a COSPAR publication)
www.elsevier.com/locate/asr

A review of geomagnetic cutoff rigidities for earth-orbiting spacecraft

D.F. Smart *, M.A. Shea

Air Force Research Laboratory VSBX, Space Vehicles Directorate, 29 Randolph Road, Bedford, MA 01731, USA

Received 2 December 2002; received in revised form 15 August 2004; accepted 1 September 2004

Abstract

Geomagnetic cutoff rigidities are a quantitative measure of the shielding provided by the earth's magnetic field. More precisely, geomagnetic cutoff rigidities predict the energetic charged particle transmission through the magnetosphere to a specific location as a function of direction. The generally accepted manner for determining cutoff rigidities is by the method of tracing particle trajectories in model magnetospheres. However, the trajectory-tracing process is so computer intensive that in the interest of economy, many approximations are still utilized. The use of modifications of the Störmer equation (with an appropriate magnetic coordinate system) is sufficient for many applications. However, for precise experimental measurements, cutoff rigidities determined by the trajectory-tracing method must be utilized.
Published by Elsevier Ltd on behalf of COSPAR.

Keywords: Geomagnetic cutoff rigidition; Earth-orbiting spacecraft; Magnetic field; Trajectory tracing

1. Introduction

The geomagnetic cutoff is a coordinate that describes charged particle access at any position in the magnetosphere. Geomagnetic cutoff rigidities are used to both describe the shielding effect of the geomagnetic field and to order charged particle data acquired in the magnetosphere. Charged particles traversing a magnetic field undergo a vector force that results in a curved path. When the general equation for the motion of a charged particle of mass (m) in a magnetic field (B) is expressed in three dimensional r, θ, ϕ, coordinates, the result is three simultaneous differential equations with six unknowns. See Smart et al. (2000) for more details.

$$\frac{dv_r}{dt} = \frac{e(v_\theta B_\phi - v_\phi B_\theta)}{mc} + \frac{v_\theta^2}{r} + \frac{v_\phi^2}{r}, \tag{1}$$

$$\frac{dv_\theta}{dt} = \frac{e(v_\phi B_r - v_r B_\phi)}{mc} - \frac{v_r v_\theta}{r} + \frac{v_\phi^2}{r\tan\theta}, \tag{2}$$

$$\frac{dv_\phi}{dt} = \frac{e(v_r B_\theta - v_\theta B_r)}{mc} - \frac{v_r v_\phi}{r} - \frac{v_\theta v_\phi}{r\tan\theta}. \tag{3}$$

Special case solutions can be obtained by specifying three of the six unknowns. With the advent of high speed digital computers and modern descriptions of the earth's magnetic field, cutoff rigidities can be calculated for any position in the magnetosphere. This is most often done for specific applications such as cosmic ray latitude surveys. For space applications, it is necessary to have a set of reference cutoff rigidity values for specific orbits such as for the International Space Station (Smart et al., 1999a,b,c). Even with modern computer technology, since the fundamental problem has no solution in closed form, millions of special case solutions are required to obtain a world-wide set of geomagnetic cutoff rigidities. The computational task is so formidable that the vertical cutoff rigidity is often the quantity calculated, and approximations are used to extrapolate to other directions or nearby locations.

* Corresponding author. Fax: +1 603 888 4733.
E-mail address: sssrc@msn.com (D.F. Smart).

0273-1177/$30. Published by Elsevier Ltd on behalf of COSPAR.
doi:10.1016/j.asr.2004.09.015

1.1. The dipole approximation

Störmer (1955) found that in a dipole field, there is an axial symmetric cone about a direction to the east in which charged particle access below a specified momentum is forbidden. This Störmer forbidden cone is illustrated in Fig. 1; other pertinent definitions are also identified.

Störmer found a special case solution exists (see Eq. (4)) in dipolar field geometry which describes the geomagnetic cutoff rigidity (rigidity = momentum per unit charge). Since the earth's magnetic field is basically dipolar and the physics of the Störmer equation is fundamentally sound, this equation can be applied to most space applications. The limitations are the frequent use of simplistic and imprecise approximations for magnetic latitude and the distance from the earth's effective magnetic center.

In Eq. (4),

$$R_c = [M\cos^4\lambda]/\{r^2[1+(1-\sin\epsilon\sin\xi\cos^3\lambda)^{1/2}]^2\}. \quad (4)$$

R_c is the geomagnetic cutoff rigidity (in MV), M is the magnitude of the dipole moment in G cm^3, λ is the latitude from the magnetic equator, ϵ is the angle from the zenith direction (where the zenith direction is a radial from the position of the dipole center), ξ is the azimuthal angle measured clockwise from the direction to the north magnetic pole and r is the distance from the dipole center in centimeters. (Note that this equation is in the old mixed CGS units; necessary conversion constants include 10^9 eV per GV and 300 V per Abvolt.)

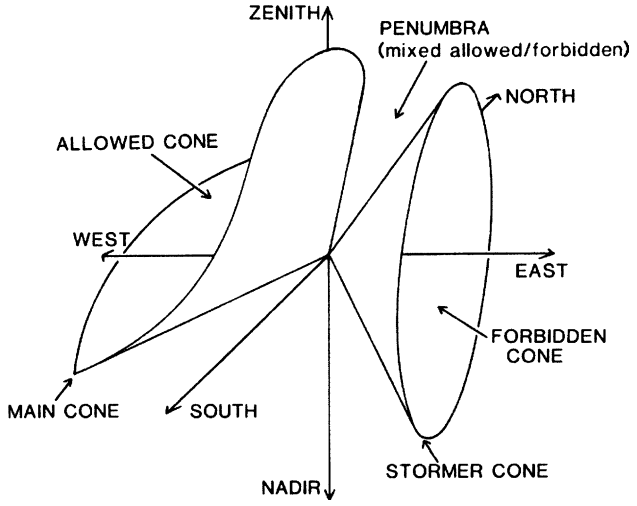

Fig. 1. Geometric visualization of cutoffs. The Störmer or forbidden cone is a right circular cone about the magnetic east direction and is an intrinsic property of a dipole field. It is defined by an exact solution of the Störmer (1955) integral. The main cone is a concept developed by Lemairte and Vallarta (1936) and is not defined by any exact equation. The cosmic ray penumbra is a chaotic region of allowed and forbidden cosmic ray access that has defied all attempts to order it. See Cooke et al. (1991) for further definitions.

The value for the dipole moment is obtained by multiplying the g_1^0 term (in units of G) of the International Geomagnetic Reference Field by the cube of the average radius of the earth (in cm). When this equation is used in normalized units, where r is expressed in earth radii and the unit of cutoff rigidity is in GV, the magnitude of the dipole moment has a value ~58 for the IGRF 2000 magnetic field model. Many texts still quote the original 1930 value derived by Störmer which ignores the evolution of the geomagnetic field. See Smart and Shea (1994) for further details.

When Eq. (4) is normalized to distance in earth radii (from the dipole position) and a "vertical" (dipole radial) geomagnetic cutoff (in units of GV) is desired, the denominator of the Störmer equation reduces to a value of 4, and the constant evaluates to ~14.5 for the IGRF 2000 magnetic field as shown in Eq. (5)

$$R_{cv} = (14.5\cos^4\lambda)/r^2. \quad (5)$$

In using this equation the corrected geomagnetic latitude (Gustafsson, 1970; Gustafsson et al., 1992) updated to the current epoch, or the invariant latitude, Λ, (derived from the McIlwain (1961) "L" coordinate updated to the current epoch, $\Lambda = \operatorname{acos}(1/\sqrt{L})$), can produce quite useful geomagnetic cutoff rigidity values. For many space applications in the earth's magnetosphere where the Mcllwain "L" coordinate has been calculated, a modified form of Eq. (5) which automatically takes into account the distance from the effective magnetic center is very useful. In Eq. (6) the constant has been normalized for the IGRF 2000 magnetic field. However, due to the non-dipole terms in the geomagnetic field, the value of the constant can range from ~14 to ~16 at various equatorial and mid-latitude positions.

$$R_{cv} = (14.5)/L^2. \quad (6)$$

In the polar latitudes, additional magnetospheric effects become important. Ogliore et al. (2001) found in the rigidity range from ~0.5 to ~1.7 GV a modified form of the above equation provided a very good ordering of the cosmic ray nuclei and solar particle data acquired by the SAMPEX spacecraft as

$$R_{cv} = 15.062\cos^4(\Lambda) - 0.363. \quad (7)$$

2. Geomagnetic cutoff rigidities determined from the IGRF models

The International Geomagnetic Reference Field models (Sabaka et al., 1997) generated under the auspices of IAGA are current state-of-the-art representations of the earth's internal magnetic field. Precise geomagnetic cutoff rigidities can be obtained by the brute force application of massive digital computer power by tracing the orbits of cosmic ray trajectories

in a model of the earth's magnetic field. Cosmic ray trajectories can be calculated at a specific direction (often the vertical for economy of computer time) for each location until there has been a reasonable sample at various rigidities and the cutoff values can be determined. Fig. 2 is an example of this trajectory-tracing process. The offset of the magnetic center with respect to the geocenter greatly complicates the geomagnetic cutoff problem.

Trajectories that would normally be allowed in a pure magnetic field become forbidden due the presence of the solid object (the earth). High rigidity cosmic rays, (such as the trajectory labeled 1), travel relatively simple orbits. As the rigidity of the particle decreases the amount of geomagnetic bending increases (examine the trajectories labeled 4 and 5) and the orbits become more complicated, forming intermediate loops. When these loops intersect the solid earth, the orbits are forbidden. At still lower rigidities, there may be allowed trajectories; trajectory 15 is an allowed orbit. The complex structure of allowed and forbidden orbits form the cosmic ray penumbra.

A common misconception is that geomagnetic cutoffs are "sharp". The general case is that the geomagnetic cutoff is "diffuse", except for the special case of geomagnetic cutoffs near the magnetic equator. There are rigidities (energies) above which all charged particles are allowed; and there are rigidities (energies) below which all charged particles are forbidden. However, in most cases, the transmission of charged particles decreases from fully allowed to totally forbidden over a discrete and often surprisingly large range of charged particle rigidities. The region between full access and totally forbidden is called the cosmic ray penumbra (a term adapted from optics). A representation of the cosmic ray penumbra is presented in Fig. 3. The cosmic ray penumbra is a chaotic region of allowed and forbidden trajectories lying between the upper computed cutoff (R_U) and the lowest computed cutoff (R_L). There are both "stable" and "unstable" regions of the cosmic ray penumbra. The "stable" regions of the cosmic ray penumbra generally contain simple orbits while the "unstable" region generally consists of long complex orbits. The cosmic ray penumbra and the directional effect of the geomagnetic cutoff frustrate the desire to obtain a simple useful number to quantify the geomagnetic cutoff effect. Effective geomagnetic cutoffs (R_C) are obtained by allowing for the transparency of the penumbra. These effective cutoffs in the vertical direction has limitations and Clem et al. (1997) found it necessary to average the cutoffs in many directions to properly describe the cosmic ray latitude curve.

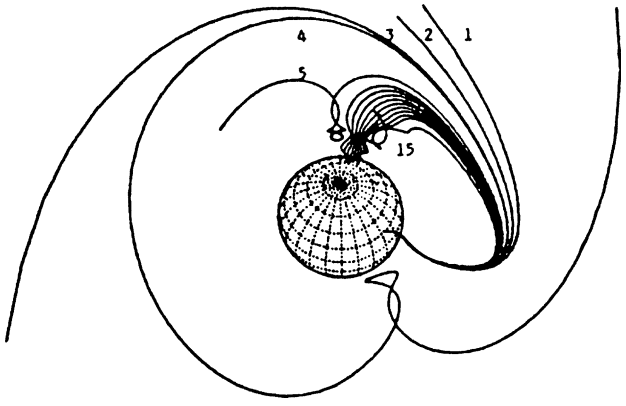

Fig. 2. Illustration of the cosmic ray trajectory-tracing process. The highest rigidity (most resistant to geomagnetic bending) is labeled 1 and the lowest rigidity is labeled 15.

2.1. Accuracy of the cutoff models at low and mid-latitudes

The accuracy of the cutoffs derived by the cosmic ray trajectory-tracing method is limited by the accuracy of the geomagnetic field model employed. A general statement is that the larger the magnitude of the cutoff, the more accurate the calculation. The cutoff values derived from cosmic ray trajectory calculations in high order simulations of the geomagnetic field at low and mid latitudes are accurate to within a "few" percent. Cosmic ray experiments have been designed purely on the basis of the cutoff rigidity calculations in the IGRF field models (Dryer and Meyer, 1975). There are very few "precision" verifications of the accuracy of the cutoff rigidity models, i.e., an absolute precision of better than one percent. There are a number of relative accuracy checks such as reproducing the latitude effect, the east–west effect and comparison with "measured" geomagnetic cutoffs. The best available verifications of cosmic ray cutoffs show that the trajectory-derived cutoffs calculated in high order simulations of the internal geomagnetic field are about 3% higher than the spacecraft-measured cutoffs at rigidities >2 GV during magnetically quiet times.

2.2. Precision checks on the geomagnetic cutoff at 400 km

The French–Danish cosmic ray experiment on the HEAO-3 satellite could record the energy, charge and direction of every cosmic ray heavy nuclei observed in its approximately one square meter collecting area. These data allowed for a check of the prediction made by tracing cosmic ray trajectories through model magnetic fields and also allowed for a verification of the accuracy of the cosmic ray cutoffs obtained by the trajectory-tracing procedure. Of particular interest were the pre-launch calculations that cosmic ray nuclei would be allowed at angles below the direction to the optical horizon at satellite altitudes. Within the experimental accuracy of the instrument, all the predictions regarding

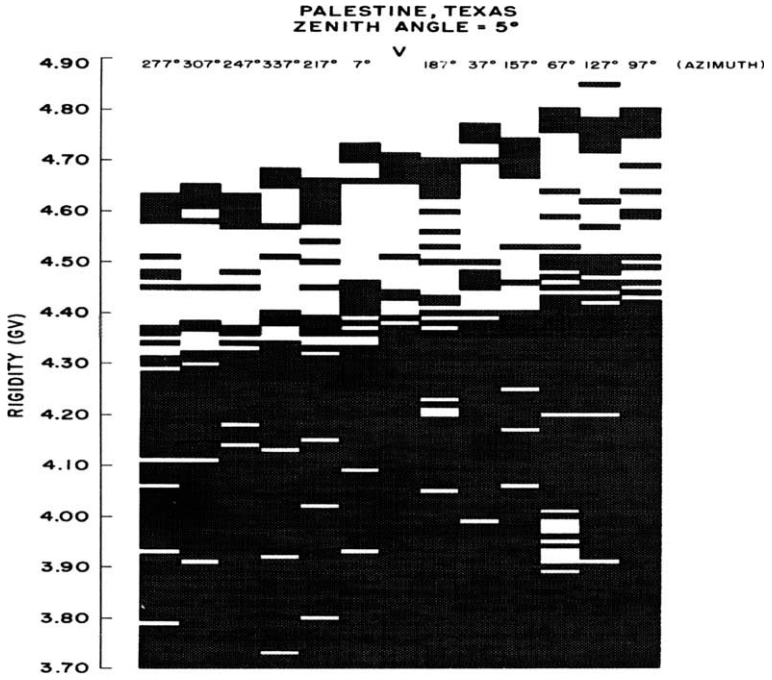

Fig. 3. Illustration of the geomagnetic cutoff transition from allowed to forbidden access as determined by cosmic ray trajectory calculations in a high order simulation of the earth's magnetic field. In this illustration black indicates forbidden rigidities and white indicates allowed rigidities. Note that the cutoff is not sharp and that as the rigidity is decreased, the transmission of cosmic rays changes from fully allowed at rigidities above the upper computed cutoff, R_U to partly allowed in the cosmic ray penumbra, to totally forbidden at rigidities below the lowest computed cutoff, R_L.

cosmic ray access to an orbiting spacecraft were verified by this experiment. The experimentally determined solid angle of cosmic ray access is illustrated in Fig. 4.

These types of data allowed for comparisons between experimentally observed and theoretically computed features of cosmic ray access to orbiting spacecraft. The trajectory calculations initially predicted that the cosmic ray penumbra would have a characteristic feature of stable bands of allowed and forbidden access. This feature has been observed by both balloon and spacecraft experiments. There is stable structure in the cosmic ray penumbra, a consistent band of forbidden orbits near the upper cutoff that was utilized by the HEAO-3 experimenters for isotopic abundance separation. The stable features in cosmic ray access through the geomagnetic field also provides for a precision check of the accuracy of the cosmic ray cutoffs determined by trajectory calculations in a model magnetic field. Comparison of the experimental and computed cutoffs in the 5 GV range from an analysis of 1885 oxygen nuclei indicates the calculated cutoffs were about 3% high. Fig. 5 illustrates the differences between the predicted cutoff (solid line) and the actual observations (dashed line).

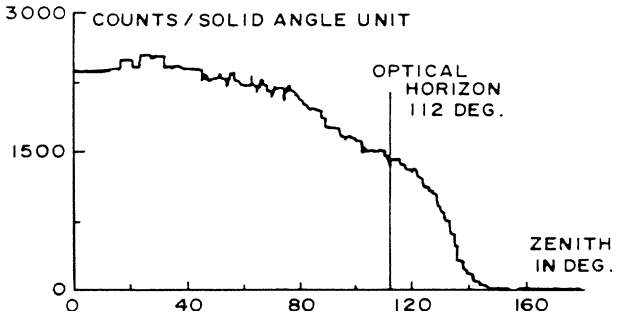

Fig. 4. A plot of the frequency of ~5 GV cosmic ray heavy nuclei observed on the HEAO-3 satellite in the zenith-west plane (Byrnak et al., 1981). These experimental results match the pre-launch predictions of the cosmic ray trajectory calculations almost perfectly. These results also match the prediction of Störmer theory.

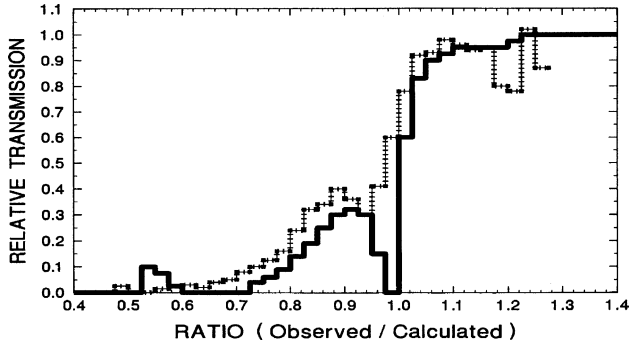

Fig. 5. Comparison between the predicted (by the trajectory-tracing procedure) and observed transition from allowed to forbidden transmission in the 5 GV geomagnetic cutoff region. The heavy solid line indicates the average predicted theoretical cutoff transition and the dashed line indicates the average observed cutoff transition. (The Copenhagen-Saclay Collaboration for HEAO, 1981).

2.3. Interpolation to other altitudes

Comparisons between the trajectory determined cutoffs and the "L" parameter (McIlwain, 1961) indicate that the approximation of Eq. (5) is very good (Shea et al., 1985) provided that both parameters are calculated using the same magnetic field model. We use this relationship for interpolation to positions within each world grid (using independent normalizations at each grid position) and also for altitude interpolation at any specified coordinate (see Fig. 6).

3. The effect of the earth's magnetosphere on geomagnetic cutoffs

The external current systems present in the earth's magnetosphere are additional magnetic sources that affect (generally reduce) the cutoff rigidity at high latitudes on the earth. The effect of these external current systems become increasingly important at rigidities below 2 GV. The generally accepted method of accounting for the magnetospheric current systems is to add a magnetospheric field model to the IGRF magnetic field model. A number of magnetospheric models have been developed, and the availability of these different models offer choices for use in a specific application. We have used the Tsyganenko (1989) magnetospheric field model combined with the International Geomagnetic Reference Field for Epoch 1995.0 (Sabaka et al., 1997) as the basis for calculating a set of world grids of vertical cutoff rigidities. The Tsyganenko (1989) magnetospheric field model was used to describe the magnetospheric field topologies for Kp magnetic indices from 0 to 5. We used the Boberg et al. (1995) extension to describe the magnetospheric fields for magnetic activity levels exceeding Kp values of 5. For convenience we labeled these as Kp 6 through 10 in Dst increments of −100 nT. Using this combined IGRF internal magnetic field and the magnetospheric model, we have computed, by the trajectory-tracing process, a complete set of world grids of vertical cutoff rigidities each 5° in latitude and 5° in longitude for a spacecraft orbiting at 450 km. This reference set of world grids of cutoff rigidities covers all magnetic activity levels from super quiet to extremely disturbed (i.e., Kp indices ranging from 0 to 9^+). For the past several years we have been working to improve the time resolution and now have world grids of vertical cutoff rigidities at 450 km for every 2 h in universal time. We will use this library of world grid cutoff rigidity calculations to illustrate the magnetospheric effects on cutoff rigidities. As an example, Fig. 7 shows some of the changes in cutoff rigidity contours between low (Kp = 0) and high (Kp = 8) levels of magnetic activity. This figure illustrates that during magnetic disturbances, the polar latitude values are greatly reduced while the mid and equatorial latitude cutoffs undergo only moderate reductions. Note the change in the latitude of the 1 GV contour and the disappearance of the 15 GV contour at the Kp = 8 magnetic activity level in the right panel.

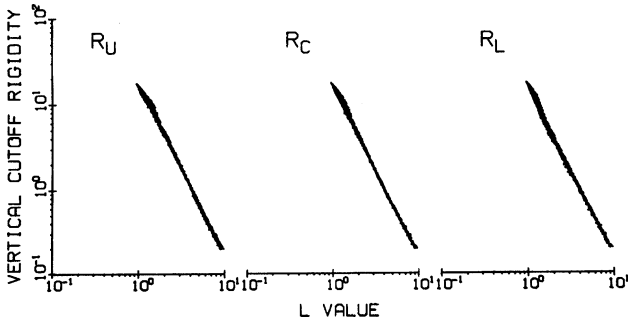

Fig. 6. Illustration of the relationship between the McIlwain L parameter and trajectory-derived vertical geomagnetic cutoffs. The slope of the lines is -2.00 ± 0.05. R_U is the upper computed cutoff, R_L is the lowest computed cutoff, and R_C is the effective cutoff rigidity.

Rigidity (momentum per unit charge) is not the most convenient unit for use with energetic particle data since most energetic particle measurements are in units of energy. For comparison purposes, we have selected the invariant latitude calculated from the internal geomagnetic field as a common parameter. We have obtained an average invariant latitude for each cutoff energy as shown in Fig. 8. This figure again illustrates that during magnetic disturbances, the polar latitude values are greatly reduced while the mid and equatorial latitude cutoffs undergo only moderate reductions. These curves indicate an almost linear relation between the proton cutoff energy with latitude in the range from about 10 MeV to a few 100 MeV. We note that the change of proton cutoff energy with Kp is relatively uniform over the range of the original Tsyganenko (1989) model, but the cutoff changes introduced by the Boberg et al. (1995) extension is non-linear with the Dst increment.

3.1. Comparison with spacecraft proton cutoff measurements

We have compared these computed average invariant latitudes of these predicted average solar proton cutoff latitudes with the SAMPEX spacecraft measured cutoff latitudes (see Fig. 9) published by Leske et al. (1997). This figure shows that the cutoff latitudes derived from interpolation through our library of magnetospheric cutoffs and measured cutoff latitudes exhibit the same general trend. During magnetically active times the "measured" cutoff latitudes are slightly lower and show more detailed structure than the 3-h averaged, Kp indexed, interpolated vertical geomagnetic cutoffs.

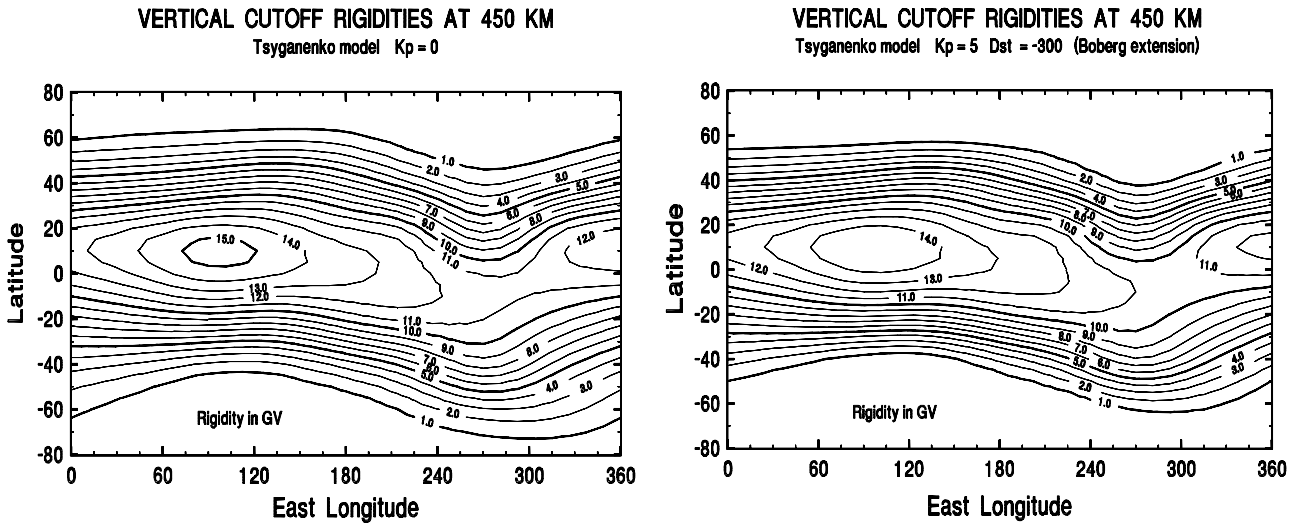

Fig. 7. Contour maps of universal time averaged computed vertical cutoff rigidities for a 450-km orbiting spacecraft for quiet (Kp = 0 on the left), and disturbed (Kp = 8 on the right) magnetic conditions. The cutoff rigidity contours are in GV increments. The maximum cutoff rigidities are along the magnetic equator and the minimum cutoff rigidity is at the magnetic poles.

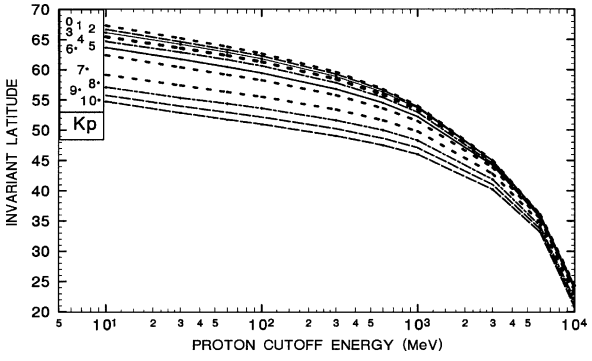

Fig. 8. Proton effective vertical cutoff energy at 450 km as a function of magnetic activity.

4. Application of geomagnetic cutoff rigidities to radiation dose calculations

Geomagnetic cutoff rigidities predict the energetic charged particle transmission through the magnetosphere to a specific location as a function of direction. The STS28 space shuttle flight in August 1989 carried a dosimeter that provided data during the onset of the large solar proton event sequence that began on 12 August 1989. We have used the dosimetry data acquired during the actual space flight as a method of evaluating the accuracy of the cutoff rigidities derived from the combined IGRF-Tsyganenko (1989) magnetospheric model. During the time the vehicle encountered solar protons,

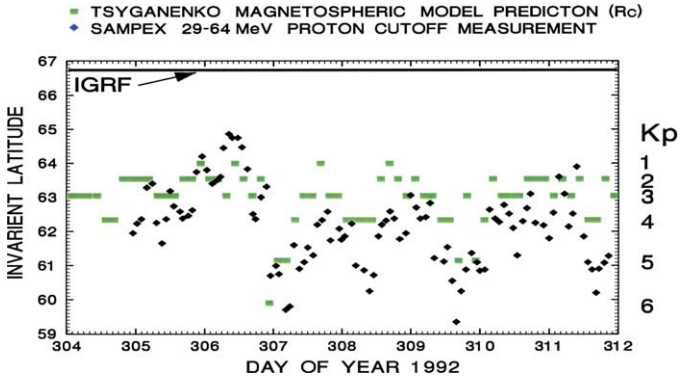

Fig. 9. Simulation of the invariant latitude of the proton cutoff energy variations as a function of the Kp index. The solid dark line at 67.5° indicates the cutoff latitude predicted by the internal IGRF magnetic field model (Smart and Shea, 1997). The gray solid squares indicate the predicted cutoff invariant latitude for the center energy of the 29–64 MeV detector on the SAMPEX spacecraft. The solid diamonds are the cutoff latitudes published by Leske et al. (1997). The cutoff latitude for each Kp value is indicated on the left of the figure and the integer Kp values are on the right.

the geomagnetic activity level as quantified by the Kp index varied between 1 and 3. We used the dynamic cutoff rigidity model to predict the solar proton transmission through the magnetosphere to the position of the space shuttle (latitude, longitude and altitude) each minute of the shuttle fight during its encounter with the solar proton event. The solar proton flux predicted to penetrate the geomagnetic field and arrive to the skin of the space shuttle was used as input to the NASA/JSC PDOSE code to compute the radiation dose rate. A more detailed description of this radiation dose rate calculation method is given by Golightly and Weyland (1997).

The STS28 dose rate data set also provided an opportunity to check the applicability of the various cutoff rigidity parameters such as R_U, R_L, and R_C. We found that truncating the Kp magnetic activity index results in a cutoff value at the spacecraft position that is too high and the solar particle flux predicted to be allowed at the spacecraft is not sufficient to reproduce the dose measurement. It is necessary to "round up" the Kp index in order to obtain a cutoff value that predicts a dose rate that is consistent with the measured dose rate. Our results show.

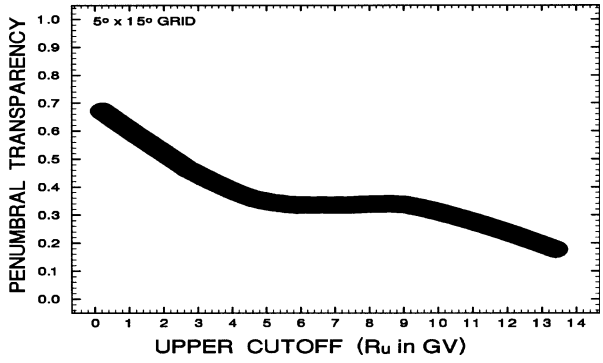

Fig. 10. Average transmission of charged particles through the penumbra found by averaging the penumbra transparency values in the 450 km world grid of cutoff rigidities by GV intervals.

1. Use of the upper cutoff rigidity, R_U, resulted in an underprediction of the dose rate.
2. Use of the lower cutoff rigidity, R_L, resulted in an overprediction of the dose rate.
3. Use of the effective cutoff rigidity, R_C, resulted in a slight systematic underprediction of the dose rate.
4. Using all of the solar proton flux down to R_U and then using the average transparency of the penumbra to specify the solar particle flux transmitted through the penumbra between R_U and R_L resulted in a systematically better correspondence between the computed and measured dose rate. This average transparency, a function of the cutoff rigidity, is shown in Fig. 10.

It was necessary to include the effect of the lower cutoffs in the western direction (derived by the application of Störmer theory) to reproduce the observed radiation dose intensity/time profile. The allowed solid angle of particle access to the spacecraft was divided into five equal solid angle segments: vertical, north, south, east and west. The particle flux allowed though the geomagnetic cutoff for each individual segment was summed to find the allowed particle flux over the solid angle of particle access. Employing the dynamic cutoff rigidity model with a proper selection of the magnetic activity index resulted in a one-to-one correspondence between the time periods of computed radiation dose rate due to solar protons being allowed through the magnetosphere to the position of the space shuttle and the measured dose rate in the vehicle, even for very small doses. Employing the solar proton flux spectra and the appropriate Kp magnetic activity indices enabled the computation of the solar particle dose rate for each minute of the STS28 flight. The comparison between the computed and measured dose rate is given in Fig. 11. A more detailed description of these results are given by Smart and Shea (2002) and Smart et al. (2003).

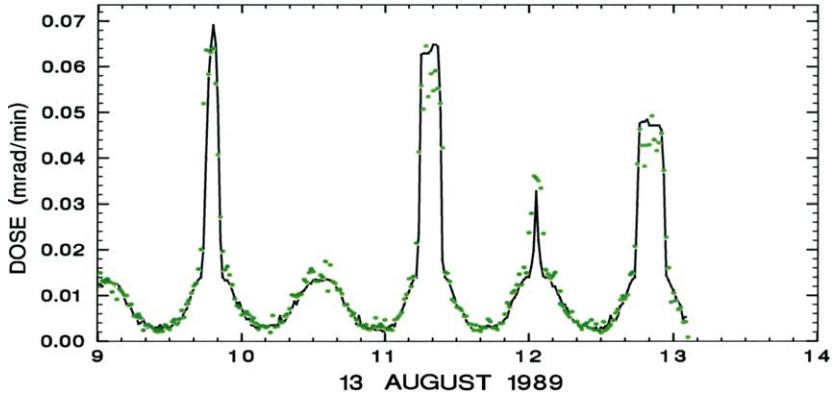

Fig. 11. Comparison of computed (solid line) and observed (dots) radiation dose rate during the 13 August 1989 solar proton event.

5. Summary

Geomagnetic cutoff rigidities are a quantitative measure of the shielding provided by the earth's magnetic field. However, there is no simple number that completely describes the geomagnetic cutoff. Instead, at each position and in each direction there are three distinct quantities that describe the geomagnetic cutoff. These are:

R_U, the upper cutoff value.
R_L, the lower cutoff value.
R_C, the effective cutoff value.

The "effective" cutoff value is used for many applications because it satisfies the desire to have a simple value for the geomagnetic cutoff rigidity. This simple value has limitations and we have found that for precision spacecraft measurements, it gives a systematic offset to the results. We have found it necessary to specifically account for the particle transmission through the penumbral region when attempting to match precision spacecraft particle measurements. We also found it necessary to consider the geomagnetic cutoff in each direction (more properly, a computation of the solar particle flux allowed in each direction) to reproduce spacecraft dosimetry data during a solar particle event.

The accepted manner for determining cutoff rigidities is tracing particle trajectories in a current International Geomagnetic Reference Field model in combination with a model magnetosphere. Cutoff rigidities derived from the IGRF models are accurate to a few percent in the multi GeV region. The addition of magnetospheric models improves the accuracy at low energies (<1 GeV). However, the trajectory-tracing process is computer intensive; many approximations are still utilized. We have found that the use of modifications of the Störmer equation (*with an appropriate magnetic coordinate system*) is sufficient for many applications.

6. Additional comment

The cutoff rigidity values described in this paper have been incorporated into a geomagnetic cutoff interpolation model designated as AFRCIUT6. This is now part of the AF-GEOSPACE suite of software programs for space environment specification. Copies of AF-GEOSPACE, Version 1.5 can be obtained by letter request to AFRL (VSBX), Hanscom AFB, MA 10731-300, USA.

Acknowledgments

The trajectory calculations were made at the Maui High Performance Computer Center. We thank M.J. Golightly, M. Weyland, A.S. Johnson and T. Lin of the NASA Johnson Space Center for providing the STS28 radiation dose data and assistance with the SPERT radiation dose code.

References

Boberg, P.R., Tylka, A.J., Adams, J.H., Flückiger, E.O., Kobel, E. Geomagnetic transmission of solar energetic protons during the geomagnetic disturbances of October 1989. Geophys. Res. Lett. 22, 1133–1136, 1995.

Byrnak, B., Lund, N., Rasmussen, I.L., Petrou, N. The isotopic composition of cosmic ray nuclei at 0.6, 3 and 7 GeV/n. Proc. 17th Int. Cosmic Ray Conf. 2, 11–18, 1981.

Clem, J.M., Bieber, J.W., Duldig, M., Evenson, P., Hall, D., Humble, J. Contribution of obliquely incident particles to neutron monitor counting rate. J. Geophys. Res. 102, 26919–26926, 1997.

Cooke, D.J., Humble, J.E., Shea, M.A., Smart, D.F., Lund, N., Rasmussen, I.L., Byrnak, B., Goret, P., Petrou, N. On cosmic-ray cut-off terminology. Il Nuovo Cimento 14, 213–234, 1991.

Copenhagen-Saclay The HEAO-3 French Danish cosmic ray spectrometer: preliminary results of the elemental abundances of cosmic ray nuclei in the iron peak. Adv. Space Res. 1, 173–184, 1981.

Dryer, R., Meyer, P. Isotopic composition of cosmic-ray Nitrogen at 1.5 GeV/AMU. Phys. Rev. Lett. 35, 601–604, 1975.

Golightly, M.J., Weyland, M. Modeling exposures aboard the space shuttle from the August 1989 Solar Particle Event, Paper No. 13 in Impact of solar energetic particle events on design of human missions, Center for Advanced Space Studies, Houston, TX, 1997.

Gustafsson, G. A revised corrected geomagnetic coordinate system. Arkiv. Geofysik. 5, 595–617, 1970.

Gustafsson, G., Papitashvilli, N.E., Papitashvilli, V.O. A revised corrected geomagnetic coordinate system for Epochs 1985 and 1990. J. Terr. Phys. 54, 1609–1631, 1992.

Lemairte, G., Vallarta, M.S. On the allowed cone of cosmic radiation. Phys. Rev. 50, 493–504, 1936.

Leske, R.A., Mewaldt, R.A., Stone, E.C., von Rosenvinge, T.T. Geomagnetic cutoff variations during solar energetic particle events – implications for the space station. Proc. 25th Int. Cosmic Ray Conf. 2, 381–384, 1997.

McIlwain, C.E. Coordinates for mapping the distribution of trapped particles. J. Geophys. Res. 66, 3681–3691, 1961.

Ogliore, R.C., Mewaldt, R.A., Leske, R.A., Stone, E.G., von Rosenvinge, T.T. A direct measurement of the geomagnetic cutoffs for cosmic rays at space station latitudes. Proc. 27th Intl. Cosmic Ray Conf. 10, 4112–4115, 2001.

Sabaka, T.J., Langel, R.A., Baldwin, T.T., Conrad, J.A. The geomagnetic field, 1900–1995, including the large scale fields from magnetospheric sources and NASA Candidate Models for the 1995 revision of the IGRF. J. Geomag. Geoelectr. 49, 157–206, 1997.

Shea, M.A., Smart, D.F., Gentile, L.C. The use of the McIlwain *L*-parameter to estimate cosmic ray vertical cutoff rigidities for different epochs of the geomagnetic field. Proc. 19th Intl. Cosmic Ray Conf. 5, 332–335, 1985.

Smart, D.F., Shea, M.A. Geomagnetic cutoffs: a review for space dosimetry applications. Adv. Space Res. 14 (10), 787–796, 1994.

Smart, D.F., Shea, M.A. Calculated cosmic ray cutoff rigidities at 450 km for Epoch 1990.0. Proc. 25th International Cosmic Ray Conference 2, 397–400, 1997.

Smart, D.F., Shea, M.A., Flückiger, E.O. Calculated vertical cutoff rigidities for the international space station during magnetically quiet times. Proc. 26th Int. Cosmic Ray Conf. 7, 394–397, 1999a.

Smart, D.F., Shea, M.A., Flückiger, E.O., Tylka, A.J., Boberg, P.R. Calculated vertical cutoff rigidities for the international space station during magnetically active times. Proc. 26th Int. Cosmic Ray Conf. 7, 398–401, 1999b.

Smart, D.F., Shea, M.A., Flückiger, E.O., Tylka, A.J., Boberg, P.R. Changes in calculated vertical cutoff rigidities at the altitude of the International Space Station as a function of magnetic activity. Proc. 26th Int. Cosmic Ray Conf. 7, 337–340, 1999c.

Smart, D.F., Shea, M.A., Flückiger, E.O. Magnetospheric models and trajectory computations. Space Sci. Rev. 93, 305–333, 2000.

Smart, D.F., Shea, M.A. Comparison of solar particle dose calculated using the dynamic geomagnetic cutoff rigidity model with spacecraft dosimetry data, CD-ROM by American Nuclear Society 12th Biennial RPSD Topical Meeting, at Santa Fe, New Mexico, 14–18 April 2002.

Smart, D.F., Shea, M.A., Golightly, M.J., Weyland, M. Evaluation of the dynamic cutoff rigidity model using dosimetry data from the STS-28 Flight. Adv. Space Res. 31, 841–846, 2003.

Störmer, C. The Polar Aurora. Clarendon Press, Oxford, 1955.

Tsyganenko, N.A. A magnetospheric magnetic field model with a warped tail current sheet. Planet. Space Sci. 37, 5–20, 1989.